Quantum decay of the persistent current in a Josephson junction ring

D. A. Garanin and E. M. Chudnovsky
Physics Department, Lehman College, The City University of New York, 250 Bedford Park Boulevard West, Bronx, NY 10468-1589, USA
(Received 12 November 2015; published 7 March 2016)

We study the persistent current in a ring consisting of $N \gg 1$ Josephson junctions threaded by the magnetic flux. When the dynamics of the ring is dominated by the capacitances of the superconducting islands the system is equivalent to the xy spin system in $1+1$ dimensions at the effective temperature $T^* = \sqrt{2JU}$, with J being the Josephson energy of the junction and U being the charging energy of the superconducting island. The numerical problem is challenging due to the absence of thermodynamic limit and slow dynamics of the Kosterlitz-Thouless transition. It is investigated on lattices containing up to $\times 10^6$ sites. At $T^* \ll J$ the quantum phase slips are frozen. The low-T^* dependence of the persistent current computed numerically agrees quantitatively with the analytical formula provided by the spin-wave approximation. The high-T^* behavior depends strongly on the magnetic flux and on the number of superconducting islands N. We present a detailed numerical study of the unbinding of vortex-antivortex pairs responsible for the phase slips, the superconductor-insulator transition, and evolution of the persistent current in a finite-size system.

DOI: 10.1103/PhysRevB.93.094506

I. INTRODUCTION

Microscopic chains of Josephson junctions have been at the forefront of research on quantum phase transitions [1,2] and quantum circuitry [3–5]. They provide a testing field for two fundamental physical effects: quantum phase slips [6–8] and superconductor-insulator transition [9–12]. Persistent currents in small metallic rings have been studied theoretically and experimentally since the 1960s [13], while the studies of microscopic Josephson junction rings are more contemporary. They are rapidly advancing due to the progress in manufacturing the nanostructures [12].

Analytical research on Josephson junction rings focused on two limits: when the dynamics of the ring is dominated by the capacitances of the junctions [14] and when the dynamics is dominated by the capacitances of the superconducting islands [15]. Also the mixed situation with both capacitances has been studied. The persistent currents were computed numerically for the rings containing up to 40 superconducting islands [16], as well as analytically using the effective low-energy description [8]. Quantum phase slips in a Josephson junction chain have been studied experimentally [17] and good agreement with theoretical concepts [14] has been demonstrated.

Our interest in the problem has been motivated by the strong size effect observed in the previous numerical studies of the persistent currents in relatively small Josephson junction rings (Fig. 1). It demonstrated the necessity to study longer chains with a large number of superconducting islands N. The case when the dynamics of the ring is dominated by the capacitances of the islands, which is considered here, permits such large-N analysis because the quantum one-dimensional (1D) problem of the ring maps onto a classical 2D xy spin model at a finite temperature that is well suited for large-scale Monte Carlo (MC) studies.

Our approach is largely based upon the ideas that go back to the work of Choi [15] who studied analytically the persistent current dominated by the capacitances of the superconducting islands. There is also a more recent detailed analytical study of the persistent current in the general case of finite capacitances of the junctions in addition to capacitances of the superconducting islands [8]. The focus of these and other works has been on the thermodynamic limit, while we focus on a large-scale numerical study of finite-size effects and contributions of topological objects to the formation of the persistent current. Such studies are especially important in the case of strong quantum fluctuations not accessible quantitatively by analytical methods.

The equilibrium persistent current in a Josephson junction ring threaded by the magnetic flux depends on the value of the flux. It may be destroyed by temperature or by quantum fluctuations. The measure of the strength of quantum fluctuations is the ratio of the charging energy of the superconducting island, U, and the Josephson coupling between the islands, J. Exact mapping of the problem onto the 2D xy spin problem allows one to express the effect of quantum fluctuations at zero temperature in terms of the effective "quantum" temperature $T^* = \sqrt{2JU}$. The Kosterlitz-Thouless (KT) temperature, $T_{\rm KT} \sim J$, at which the quasi-long-range order in the 2D model is destroyed provides the critical value of U that results in the superconductor-insulator transition.

When the flux is different from $(n+1/2)\Phi_0$, where n is an integer and Φ_0 is the flux quantum, the equilibrium persistent current has a nonzero value as long as quantum fluctuations are weak, $T^* < T_{\rm KT}$. With increasing quantum fluctuations one should expect the persistent current to become zero at $T^* = T_{\rm KT}$. The situation is more complicated in the half-fluxon case, $\Phi = (n+1/2)\Phi_0$, when quantum phase slips provided by vortices of the 2D xy classical model connect, via quantum tunneling, the states with persistent currents running in opposite directions. In this case the MC routine elucidates the fact that while the persistent current is theoretically metastable at any nonzero U, the phase slips are frozen at $T^* \ll T_{\rm KT}$, making small Josephson junction rings to resemble superparamagnetic particles.

The numerical solution of the problem is challenging in comparison with the typical problems of magnetic phase transitions for two reasons. First, the persistent current is a mesoscopic quantity that becomes small for a large system size, $I \propto 1/N$. This is why the increase in the system size

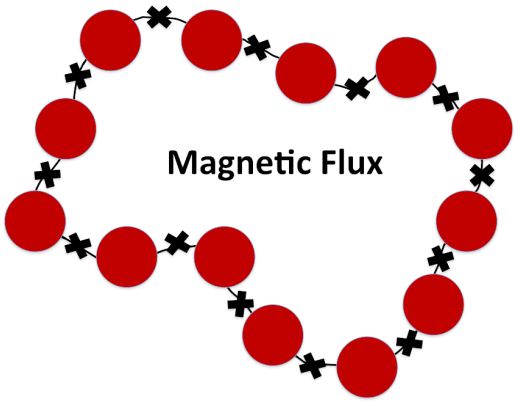

FIG. 1. A ring of N Josephson junctions (crosses) made of superconducting grains (circles), threaded by the magnetic flux.

does not lead to a significant improvement of the results via self-averaging. At high quantum temperatures the root-mean-square fluctuations of the persistent current, $\sqrt{\langle I^2\rangle} \propto 1/N$, decrease with the size but so does the current itself. The second reason is that the (pseudo)dynamics of vortices is extremely slow. It requires a large number of updates and computer runs.

The paper is structured as follows. The theory is given in Sec. II. The model of a Josephson junction ring whose dynamics is dominated by capacitances of superconducting islands is formulated in Sec. II A. The equivalence of the model to the xy spin model in 1+1 dimensions at finite temperature is reviewed in Sec. II B. Persistent current and its T^* dependence expected from the theory are discussed in Sec. II C. Numerical results are presented in Sec. III. The numerical method is described in Sec. III A. The formation of vortices responsible for the phase slips and for quantum KT transition is discussed in Sec. III B. In Sec. III C we present numerical results on the destruction of the persistent current by quantum fluctuations. The energy barrier for the phase sleep is analyzed in Sec. IV. Section V contains some final remarks and suggestions for experiment.

II. THEORY

A. Ring made of Josephson junctions

Consider a Josephson junction ring depicted in Fig. 1. Let θ_j be the phase of the superconducting order parameter $\Psi = |\Psi|\exp(i\theta)$ at the jth superconducting island. The Josephson energy of the ring is then given by [18]

$$E_J = J\sum_i \left[1 - \cos\left(\theta_{i+1} - \theta_i + \frac{2\pi}{\Phi_0}\int_i^{i+1} \mathbf{A}\cdot d\mathbf{l}\right)\right], \quad (1)$$

where the vector potential $\mathbf{A}$ is due to the magnetic flux Φ piercing the ring.

The summation along the closed loop of the ring gives

$$\sum_i \left(\theta_{i+1} - \theta_i + \frac{2\pi}{\Phi_0}\int_i^{i+1} \mathbf{A}\cdot d\mathbf{l}\right) = 2\pi(\phi + m), \quad (2)$$

where $\phi \equiv \Phi/\Phi_0$, $\Phi_0 = h/(2e)$ is the flux quantum, and m is an arbitrary integer. This can be derived by computing the flux through the ring as $\Phi = \oint \mathbf{A}\cdot d\mathbf{l}$ and noticing that the superconducting current $\mathbf{j}_s = \frac{e\hbar}{m}|\Psi|^2(\nabla\theta - \frac{2\pi}{\Phi_0}\mathbf{A})$ is zero inside the islands since we only have Josephson currents between the grains in the system.

Equation (2) allows one to write

$$E_J = J\sum_i \left[1 - \cos\left(\tilde{\theta}_{i+1} - \tilde{\theta}_i + \frac{2\pi(\phi + m)}{N}\right)\right], \quad (3)$$

where the reduced phases $\tilde{\theta}$ are defined in such a way that the change of $\tilde{\theta}_i$ around the ring is zero. The total change in the original phase θ accumulated around the ring is accounted for by the quantum number m. These reduced phases are convenient for the analytical work, whereas the numerical work uses the original phases. The energy minimum corresponds to all reduced phases being the same, leading to the ground state

$$E_J^{(0)} = NJ\left[1 - \cos\left(\frac{2\pi(\phi + m)}{N}\right)\right] \cong \frac{(2\pi)^2 J}{2N}(\phi + m)^2, \quad (4)$$

the last expression being the large-N case. Branches of $E_J^{(0)}(\Phi)$ for different values of m are shown in Fig. 2(a). When $\phi = n + 1/2$, with n being an integer, that is, for $\Phi = (n + 1/2)\Phi_0$, the ground state is degenerate, $E_J(n,m) = E_J(n,m' = -2n - m - 1)$. This permits quantum tunneling between $E_J(n,m)$ and $E_J(n,m')$ that removes the degeneracy. For example, for $n = 0$, that is, when the flux equals half a fluxon, $\Phi = \Phi_0/2$ ($\phi = 1/2$), the states with $m = 0$ and $m = -1$, corresponding to different current states in the ring, have the same energy. Quantum oscillations between such states have been observed in experiment [19,20].

B. Dynamics

The dynamics of the Josephson junction ring is due to the electrical charging of the superconducting islands by the excess (or lack) of Cooper pairs n_i at the ith site. It is determined by the finite capacitances of the islands to the ground and the capacitances of the junctions. Different limits,

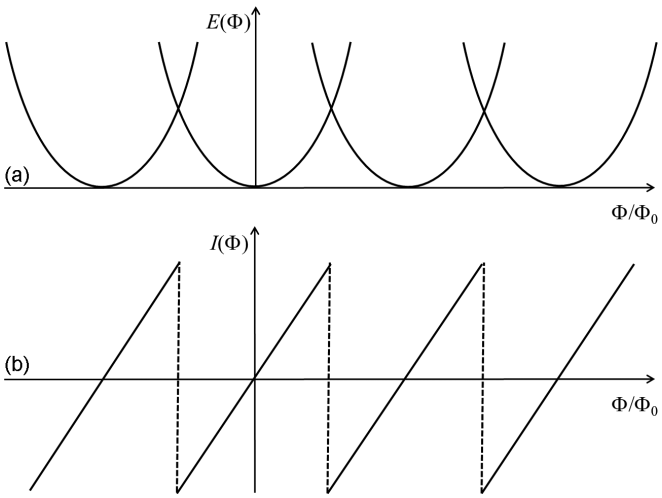

FIG. 2. (a) m branches of the ground-state energy $E_J^{(0)}$. (b) m branches of the persistent current.

with both capacitances present, can be achieved in experiment and have been studied in literature (see, e.g., Ref. [8], and references therein). In this paper we are considering the limit in which the capacitances of the islands, C, greatly exceed the capacitances of the junctions. In this case the charging energy is given by

$$E_C = \sum_i U n_i^2 = \frac{\hbar^2}{4U} \sum_i \left(\frac{d\theta_i}{dt} \right)^2, \tag{5}$$

where $U = (2e)^2/(2C)$. The second of Eq. (5), which plays the role of the kinetic energy, is obtained by noticing that n_i and θ_i are canonically conjugated variables. If they are treated quantum mechanically, one has

$$n_i = -i \frac{d}{d\theta_i}, \quad i\hbar \frac{d\theta_i}{dt} = [\theta_i, E_C] = 2iUn_i. \tag{6}$$

The Lagrangian of the model is $\mathcal{L} = E_C - E_J$, and the equations of motion are

$$\hbar \frac{dn_i}{dt} = -J \sum_j \sin \left(\theta_i - \theta_j - \frac{2\pi}{\Phi_0} \int_i^j \mathbf{A} \cdot d\mathbf{l} \right), \tag{7}$$

where the summation is over the nearest neighbors. Summing up this equation over i and noticing that swapping i and j changes the sign of the right-hand side, it is easy to see that the dynamics of the system conserves the total charge $Q = \sum_i n_i$.

Quantum mechanics of the model is formulated in terms of the path integral

$$I = \prod_i \int D\{\theta_i(\tau)\} e^{-S_E/\hbar}, \tag{8}$$

where $\tau = it$ and $S_E = \int d\tau \, \mathcal{L}$ is the Euclidean action with

$$\mathcal{L} = \frac{\hbar^2}{4U} \sum_i \left(\frac{d\theta_i}{d\tau} \right)^2 + J \sum_i \left[1 - \cos \left(\theta_{i+1} - \theta_i + \frac{2\pi\phi}{N} \right) \right]. \tag{9}$$

Here the phases θ_i are the original phases, as in Eq. (1), not the reduced phases of Eq. (3).

Note that in the presence of dissipative shunts across the junctions, the equations of motion that follow from Eq. (9) must be complemented by terms $R^{-1}[\Phi_0/(2\pi)]^2(d\Delta\theta_{ij}/dt)$, where R is the phenomenological normal resistance of the junction. At the microscopic level the dissipation can be taken into account by introducing linear interaction of Josephson phases with a continuum of harmonic oscillators [21]. This, however, would require impractically large computer times needed to obtain a persistent current. In this paper we are making the assumption that the evolution of the persistent current is determined by the phase slips rather than by conventional dissipation, which is equivalent to setting the normal resistance to infinity.

Statistical mechanics of this quantum model at $T = 0$ is equivalent [1,9,15,22,23] to the statistical mechanics of the classical model in $1 + 1$ dimensions at a nonzero temperature $T^* = \sqrt{2JU}$, described by the partition function

$$Z = \prod_i \int D\{\theta_i(\tau)\} e^{-\mathcal{H}_{1+1}/T^*} \tag{10}$$

with

$$\mathcal{H}_{1+1} = -\frac{1}{2} \sum_{\mathbf{r}\mathbf{r}'} J_{\mathbf{r}\mathbf{r}'} \cos(\theta_{\mathbf{r}'} - \theta_{\mathbf{r}} + \phi_{\mathbf{r}\mathbf{r}'}), \tag{11}$$

where $\mathbf{r}$ is a discrete two-dimensional vector $\mathbf{r} = (i,l)$ representing the space-time lattice, while $J_{\mathbf{r}\mathbf{r}'} = J$ for the nearest neighbors and zero otherwise. In the numerical work we use the $N \times N$ lattice with periodic boundary conditions that correspond to the surface of a toroid (Fig. 3). The circumference of the cross section of the toroid along the closed i direction contains N sites corresponding to N superconducting islands in the Josephson junction ring. The l direction along the length of the toroid corresponds to the imaginary time. Phase shifts are given by $\phi_{i,l;i\pm1,l} = \pm 2\pi\phi/N$ and $\phi_{i,l;i,l\pm1} = 0$. Notice that, in principle, the periodic boundary condition imposed on the imaginary time (our closed x direction) introduces a finite physical temperature into the original quantum problem, $T \sim T^*/N$. At large N the effect of that temperature on the persistent current can be ignored.

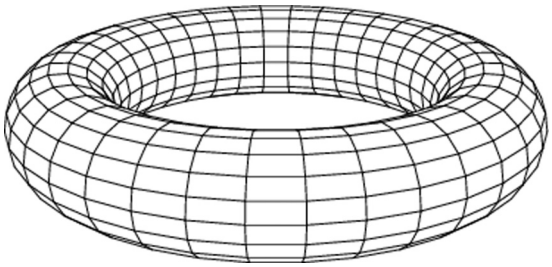

FIG. 3. $(1 + 1)$-dimensional space-time lattice with periodic boundary conditions used in numerical work.

The statistical model presented above can be reformulated in terms of the two-component classical spin vectors of the 2D xy model at temperature $T^* = \sqrt{2JU}$ that describes the strength of quantum fluctuations. As is known, the 2D xy model exhibits the Kosterlitz-Thouless phase transition at [24,25] $T_c \approx 0.89J$. For the quantum model this means that with increasing the charging energy U quantum fluctuations become sufficiently strong to destroy Josephson currents. It is believed that the corresponding quantum phase transition results in the state of the ring (sometimes called the Cooper-pair insulator) in which the islands connected by Josephson junctions maintain their superconductivity but no Josephson current can circulate in the ring. The natural way to test this interpretation of the quantum KT phase transition is to study the U dependence of the persistent Josephson current in the ring.

C. Persistent current

In accordance with electrodynamics, the persistent current in the Josephson junction ring is given by

$$I = \frac{d\langle E_J \rangle}{d\Phi} = \frac{1}{\Phi_0} \frac{d\langle E_J \rangle}{d\phi}, \tag{12}$$

where averaging is performed over quantum fluctuations with the help of the statistical model of Eq. (10). At $U = 0$, when quantum fluctuations are absent, substitution into this formula of the ground-state energy $E_J^{(0)}(\Phi)$ given by Eq. (4) results at large N in $I(\Phi)$ shown in Fig. 2(b). For example, for half a fluxon, $\Phi = \Phi_0/2$, the current has the same absolute value but flows in opposite directions for $m = 0$ and $m = -1$. Any nonzero U permits quantum tunneling between such current states that has been observed in experiment [19,20]. Equation (3) yields

$$\begin{aligned}\langle E_J\rangle &= NJ\left[1-\left\langle\cos\left(\tilde\theta_{i+1;l}-\tilde\theta_{i;l}+\frac{2\pi(\phi+m_l)}{N}\right)\right\rangle\right]\\ &= NJ\left[1-\left\langle\cos\frac{2\pi(\phi+m_l)}{N}\cos(\tilde\theta_{i+1;l}-\tilde\theta_{i;l})\right\rangle\right.\\ &\quad\left.+\left\langle\sin\frac{2\pi(\phi+m_l)}{N}\sin(\tilde\theta_{i+1;l}-\tilde\theta_{i,l})\right\rangle\right].\end{aligned}\tag{13}$$

Note that quantum fluctuations involve both fluctuations of the reduced phases $\tilde\theta_{i,l}$ and the phase slips corresponding to the tunneling transitions between different m numbers. The latter leads to different values of $m = m_l$ at different moments of the discrete imaginary time l.

At small U satisfying $T^* = \sqrt{2JU} \ll T_c \sim J$ the phase slips have exponentially small probability. Consequently, at a small T^*, if one induces a persistent current by placing the Josephson junction ring in the magnetic field, the phase slips may not occur on the time scale of the experiment. In this case the energy simplifies to

$$\langle E_J\rangle = NJ\left[1-\cos\frac{2\pi(\phi+m)}{N}\langle\cos(\tilde\theta_{i+1,l}-\tilde\theta_{i,l})\rangle\right],\tag{14}$$

since $\langle\sin(\tilde\theta_{i+1,l}-\tilde\theta_{i,l})\rangle = 0$. The persistent current computed with the help of Eq. (12) becomes

$$I = \frac{2\pi J}{\Phi_0}\sin\left(\frac{2\pi(\phi+m)}{N}\right)\langle\cos(\tilde\theta_{i,l}-\tilde\theta_{i+1,l})\rangle.\tag{15}$$

This expression corresponds to the spin-wave approximation in which the effect of the magnetic flux and the global phase change m have been factored out. In that limit it coincides with the expression for the persistent current derived in Ref. [15].

We now recall that the statistical mechanics of our model is that of the 2D xy model at $T = T^*$, for which the low-temperature (spin-wave) result is [24]

$$\langle\cos(\theta_i-\theta_{i+\delta})\rangle = 1-\frac{T^*}{4J},\tag{16}$$

δ being the nearest neighbor in any direction. This gives

$$\begin{aligned}I &= \frac{2\pi J}{\Phi_0}\sin\left(\frac{2\pi(\phi+m)}{N}\right)\left(1-\frac{T^*}{4J}\right)\\ &\cong \frac{(2\pi)^2 J}{N\Phi_0}(\phi+m)\left[1-\left(\frac{U}{8J}\right)^{1/2}\right]\end{aligned}\tag{17}$$

for the persistent current in the "spin-wave" approximation. Being interested in the limit of large N we are not studying here the periodicity [15] of the persistent current on ϕ that requires consideration of a very large magnetic flux. In the last of Eq. (17) we have used $\sin[2\pi(\phi+m)/N] \cong 2\pi(\phi+m)/N$ at large N. As we shall see, this formula agrees well with numerical results.

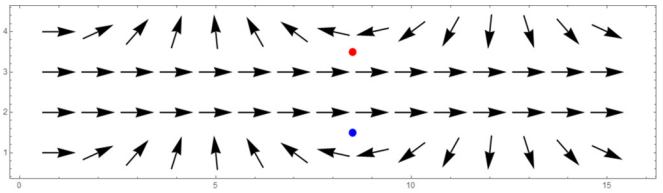

FIG. 4. Phase slip in the 2D xy model via creation of the vortex-antivortex pair.

Phase slips require creation of vortex-antivortex pairs, as is illustrated schematically in Fig. 4. The phase of each superconducting island is represented by the spin vector $\mathbf{s_r} = (\cos\theta_\mathbf{r}, \sin\theta_\mathbf{r})$. The vortex (blue dot) is shown at the center of the plaquette for which, on the way counterclockwise, the spin is rotating by 2π. For the antivortex (red dot) the spin is rotating by -2π. The horizontal direction represents the 1D ring, while the vertical direction represents the imaginary time. In the two central rows $m = 0$, while in the top and bottom rows $m = 1$. In the absence of the magnetic flux, the current in the two central rows is zero. By contrast, in the top and the bottom rows there is a current due to the phase gradient. Slow spatial rotation of the spins in these rows eventually makes them strongly noncollinear with the spins in the central rows, which, inevitably, leads to the creation of singularities—vortices and antivortices. A closely bound vortex pair has the energy of order J, thus at $T^* \ll J$ the concentration of vortex pairs is exponentially small. This is why the phase slips can be ignored in the spin-wave approximation. If the distance between the vortex and the antivortex in the pair increases, the area where the current is disturbed also increases. However, an additional energy, which is logarithmic on the separation, is required to break the pair. According to the established scenario, the vortex pairs unbind at the temperature $T^* = T_{\rm KT}$ of the Kosterlitz-Thouless transition. This would mean unlimited proliferation of the phase slips and the complete destruction of the persistent current.

In the half-fluxon case, even below the Kosterlitz-Thouless transition, vortices provide phase slips that make the persistent current tunnel between opposite directions. If one allows sufficient real or computer time, it makes the initially created persistent current evolve to the zero average corresponding to a superposition of clockwise and counterclockwise currents. It is instructive to compare the Josephson ring with the Ising system of a finite size. In the thermodynamic limit, $N \to \infty$, the 2D and 3D Ising models possess the order parameter—magnetization. This happens, because the transition from the state with the magnetization looking up to the state with the magnetization looking down requires the formation of the domain wall that traverses the system. Its energy scales as the size of the system N. By contrast, only one vortex-antivortex pair is needed for the phase slip, thus the corresponding barrier can only have logarithmic dependence on N. Consequently, one should expect that increasing the system size will not stabilize the persistent current. Thus, the latter cannot play the role of the order parameter similar to the magnetization in the

Ising model. A more detailed analysis of the barrier associated with the phase slip will be presented in Sec. IV.

III. NUMERICAL RESULTS

A. Numerical method

To solve the problem numerically, it is convenient to rewrite the effective classical Hamiltonian $\mathcal{H}_{1+1}$ of Eq. (11) in terms of the classical spin vectors $\mathbf{s_r} = (\cos\theta_\mathbf{r}, \sin\theta_\mathbf{r})$,

$$\mathcal{H}_{1+1} = -\frac{1}{2}\sum_{\mathbf{r}\mathbf{r}'} J_{\mathbf{r}\mathbf{r}'}\mathbf{s_r}\cdot\mathbb{R}_{\mathbf{r}\mathbf{r}'}\cdot\mathbf{s}_{\mathbf{r}'}, \tag{18}$$

where

$$\mathbb{R}_{\mathbf{r}\mathbf{r}'} = \begin{pmatrix} \cos\phi_{\mathbf{r}\mathbf{r}'} & -\sin\phi_{\mathbf{r}\mathbf{r}'} \\ \sin\phi_{\mathbf{r}\mathbf{r}'} & \cos\phi_{\mathbf{r}\mathbf{r}'} \end{pmatrix} \tag{19}$$

and $\phi_{\mathbf{r}\mathbf{r}'}$ are defined below Eq. (11).

Averages of physical quantities at temperature T^* are computed by a combination of standard Metropolis updates and over-relaxation. In a Metropolis update, a spin is rotated by a random trial angle and the corresponding energy change ΔE is computed. If $\Delta E < 0$, the rotation is accepted. If $\Delta E > 0$, the rotation is accepted with probability $\exp(-\Delta E/T^*)$. To keep the acceptance rate not too small and not too large, the trial angles are kept within the interval that increases with T^*. The so-called over-relaxation flips the spin over the effective field $\mathbf{H}_{\mathrm{eff},\mathbf{r}} = -\partial\mathcal{H}_{1+1}/\partial\mathbf{s_r}$ according to $\mathbf{s_r} \Rightarrow 2(\mathbf{s_r}\cdot\mathbf{h}_{\mathrm{eff},\mathbf{r}})\mathbf{s_r} - \mathbf{s_r}$, where $\mathbf{h}_{\mathrm{eff},\mathbf{r}} = \mathbf{H}_{\mathrm{eff},\mathbf{r}}/H_{\mathrm{eff},\mathbf{r}}$. Over-relaxation is, in fact, a kind of a conservative pseudodynamics. For each spin, a Metropolis update was done with the probability α and the over-relaxation was done with the probability $1-\alpha$. The constant α plays the role of the damping in our computations. This routine is performed on all spins sequentially. Updating all spins means one complete update. It is well known that for classical spin systems mixing over-relaxation with the Monte Carlo routine increases the performance of the numerical method. Metropolis updates cause dynamics of a diffusive type, making the system explore its phase space slowly. Over-relaxation is a fast ballistic process covering the phase space quickly. In our problem, pure Monte Carlo ($\alpha = 1$) does not result in switching of the current in the half-fluxon case via transitions that require creation and unbinding of the vortex-antivortex pairs. Thus, using pure Monte Carlo one can erroneously conclude that the current is stable. However, when the over-relaxation is dominant ($\alpha \ll 1$) the current is switching directions at the elevated temperatures.

Most of the numerical results were obtained with a two-stage process. First, 300 updates with $\alpha = 1$ were done to equilibrate the system's energy at a certain temperature. Then, a large number (up to 10^5) of updates with $\alpha = 0.01$ were done for each temperature to explore the phase space and to allow the switching of the current. The temperature was typically increased or decreased in small steps ($\Delta T^*/J = 0.01$) that provided an additional possibility for equilibration. Finally, similar runs of the above routine were conducted in parallel on a multicore computer and averaging over the runs was performed.

In numerical work we use the original phases of Eq. (1), represented by spin vectors. They are more convenient than the reduced phases $\tilde{\theta}_i$ since both phases and quantum numbers m are fluctuating at elevated temperatures. The average m was computed as

$$\langle m\rangle = \frac{1}{2\pi}\left\langle\sum_i(\theta_{i+1}-\theta_i)\right\rangle, \tag{20}$$

[cf. Eq. (2) that is exponentially close to an integer at low temperatures].

The software used was Wolfram *Mathematica* that allows compilation (including usage of an external C compiler that approximately doubles the speed) and parallelization. The main operating computer was Dell Precision T7610 Workstation with two Intel Xeon Processors E5-2680 v2 (10 Core, 2.8 GHz each). *Mathematica* could use 16 cores out of 20. The largest-scale computations were done for size 256^2 ($N = 256$) with 100 000 updates, size 512^2 with 10 000 updates, and size 1000^2 with 3000 updates for each temperature. The number of runs was about 100 (see indicated in figures).

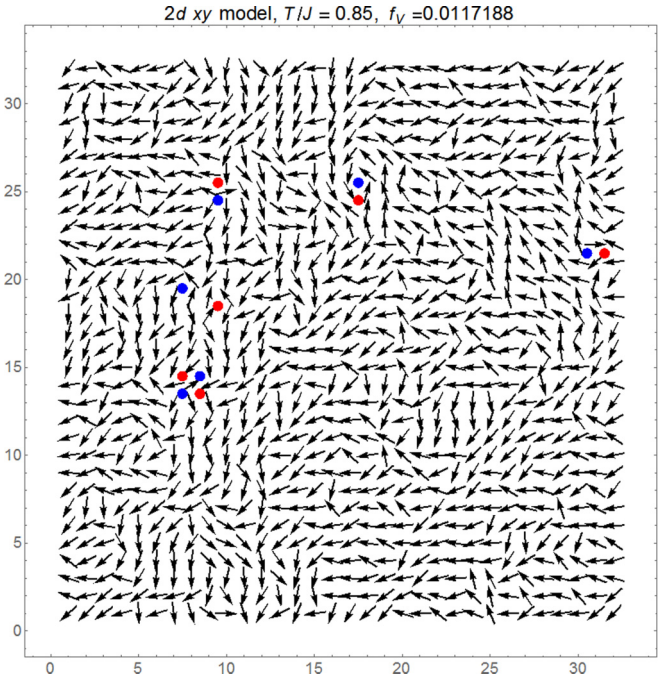

FIG. 5. Vortex pairs in the 2D xy model providing phase slips in the quantum Josephson-junction ring.

B. Vortex pairs in the effective classical 2D xy model

The underlying classical 2D xy model has been intensively studied in the past, making the Kosterlitz-Thouless transition the likely mechanism of the destruction of the persistent current by quantum fluctuations at the effective quantum temperature $T^* = T_{\mathrm{KT}}$. However, in the context of the phase slips that occur in a quantum 1D model, the numerical study of the unbinding of vortices is missing and will be presented here.

Figure 5 shows thermally excited vortex-antivortex pairs in a 2D xy system of size 32^2 at $T^*/J = 1$ that is slightly above the transition temperature at $T_{\mathrm{KT}}/J = 0.89$. One can see that vortices and antivortices are still close to each other,

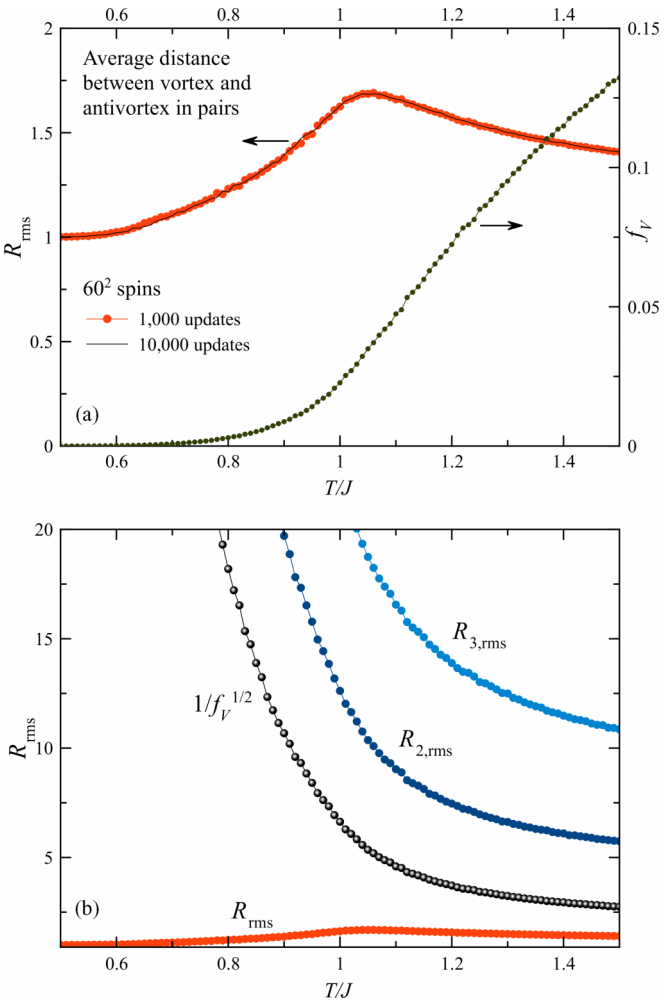

FIG. 6. Vorticity f_V and the average distance between vortices and antivortices in pairs vs T. (a) Vorticity and distance in the pairs. (b) Distances between the nearest (R_{rms}), next-nearest ($R_{2,rms}$), and next-next-nearest ($R_{3,rms}$) neighbors of a vortex, as well as the average distance between singularities $1/\sqrt{f_V}$.

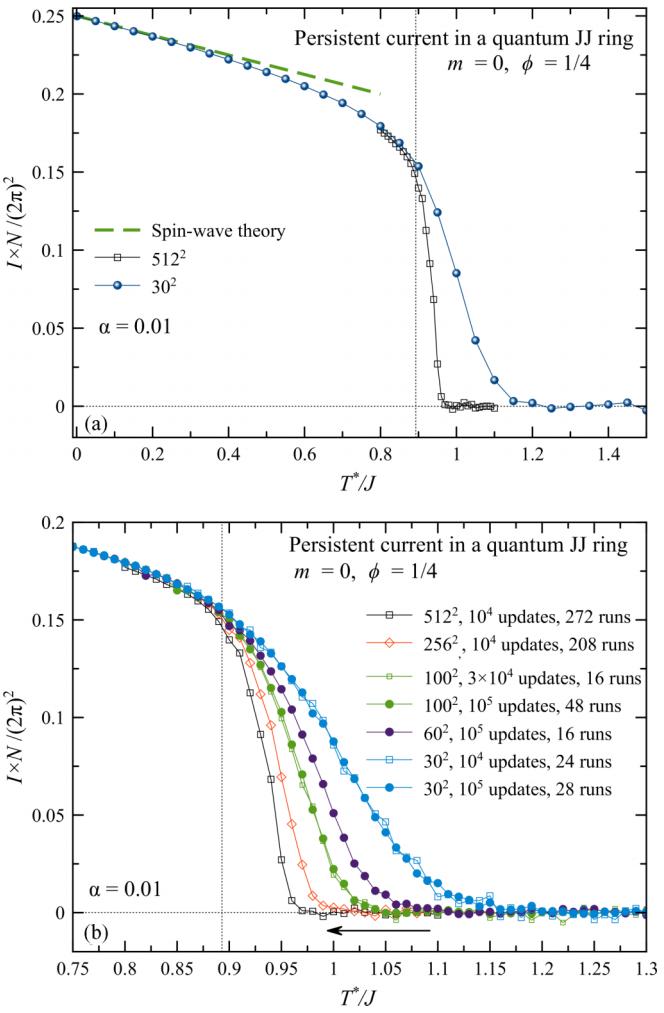

FIG. 7. Dependence of the persistent current on the quantum temperature $T^* = \sqrt{JU}$ for different lattice sizes in the quarter-fluxon case. (a) The entire temperature range. The result of the spin-wave theory is given by Eq. (17). (b) Vicinity of the Kosterlitz-Thouless transition.

although there is at least one unpaired vortex and one unpaired antivortex. Figure 6(a) shows the vorticity f_V, defined as the number of vortices and antivortices together per plaquette, for the system of size 60^2. The temperature dependence of the average root-mean-square distance R_{rms} between the vortex and antivortex in the pair is shown as well. The vorticity is exponentially small at low temperatures and it reaches the limiting value $1/3$ at $T \to \infty$. Near the KT transition the vorticity is still small, $f_V \ll 1$. The distance $R_{rms} = 1$ on the left side of the plot corresponds to the vortex and antivortex in the pair occupying neighboring plaquettes. With temperature increasing, R_{rms} increases too, as expected. Surprisingly, however, it does not become large near the KT transition, in contrast with the popular narrative of the massive production of free vortices due to the unbinding of pairs at T_{KT}. The reason for this must be that f_V increases with temperature, so that the average distance between singularities, $r^* = a/\sqrt{f_V}$, is decreasing, pressing R_{rms} down. This is illustrated in Fig. 6(b) showing R_{rms} together with the average distances to the first, second, and third nearest antivortex neighbors for a vortex in a system of size 60^2. Increasing the system size does not change these results.

C. Destruction of the persistent current by quantum fluctuations

The temperature dependence of the persistent current I in the quarter-fluxon case, $\phi = 1/4$, obtained by decreasing T^*, is shown in Fig. 7 for different system sizes N. In fact, IN is plotted. In such representation the curves for different sizes coincide everywhere except in the region of the KT transition. The spin-wave theory, Eq. (17), works well in the low-temperature region. The curves for different sizes diverge at the temperature very close to $T_{KT} = 0.89J$, becoming steeper with increasing the size. One can project that in the limit $N \to \infty$ there will be a jump at $T^* = T_{KT}$. However, in this limit the persistent current itself disappears. Since I becomes small for large sizes, its fluctuations grow and one has to perform many runs of computations to average them out. Most of the data have been obtained with 10^4 and 10^5 updates,

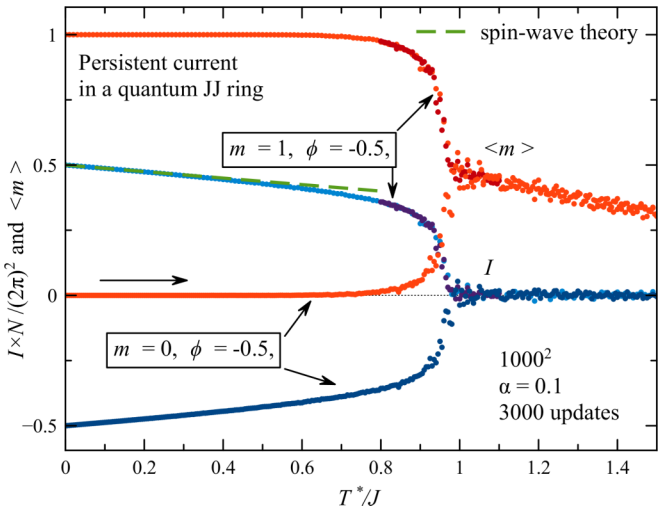

FIG. 8. Dependence of the persistent current and the average phase change $\langle m \rangle$ on increasing T^* in the half-fluxon case for the intermediate damping ($\alpha = 0.1$) and a moderate number of updates. The green dashed line is the spin-wave result of Eq. (17).

and the results for different numbers of updates coincide. This means that in our computations the system is at equilibrium at any temperature.

Results of computations for the system of size 1000^2 in the half-fluxon case, performed with the intermediate damping $\alpha = 0.1$ and a moderate number 3000 of updates for each temperature increased in small steps (without prethermalization with $\alpha = 1$), are shown in Fig. 8. At first sight $I(T^*)$ looks like the temperature dependence of the order parameter that for the biggest system size disappears at $T^*/J \approx 0.97$. The numerical data at low temperatures are very smooth and precise, while the agreement with the spin-wave theory, Eq. (17), is excellent. However, there are considerable fluctuations in a wide critical region, even for a large system size. They are related to the smallness of the current, $I \propto 1/N$. The average phase change $\langle m \rangle$ of Eq. (20) is exponentially close to an integer set as the initial condition at low temperatures. This justifies the approximation made in the derivation of Eq. (17). The temperature dependence of $\langle m \rangle$ is due to the creation and unbinding of vortex-antivortex pairs, as explained above.

Computations performed with low damping $\alpha = 0.01$ (making prethermalization with $\alpha = 1$) and a large number of updates (up to 10^5) show instability of the persistent current in the half-fluxon case, related to its tunneling between the two equal-energy classical states. In Fig. 9(a) one can see that for small system sizes I is getting destroyed by the jumping to the same-energy state well below the Kosterlitz-Thouless transition temperature. With increasing the size, the curves $I(T^*)$ are shifting to the right and saturate at size 142^2. This behavior will be explained qualitatively in the next section. Incidentally, for this size and also for $N = 256^2$ the current is disappearing exactly at $T_{\rm KT}$. This has to be taken with a grain of salt, however. Probabilities of phase slips are exponentially small, preventing the persistent current from averaging out even for 300 000 updates. This can be seen from the fact that the curves for size 256^2 in Fig. 9(b), obtained with temperature increasing, are shifting to the left when more computer time

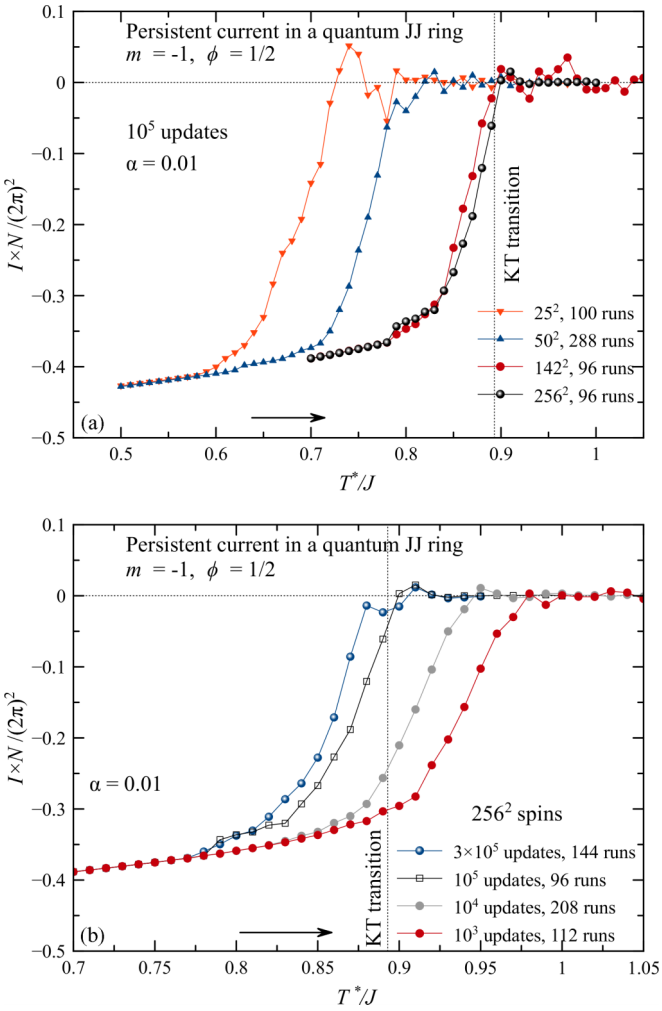

FIG. 9. Dependence of the persistent current on T^* in the half-fluxon case. (a) For different sizes with low damping ($\alpha = 0.01$) and large number of updates. (b) For different numbers of updates.

is allowed for relaxation, that is, with the number of updates. Although it would take impractically long computer time to increase the number of updates past 10^6, one can project that for a sufficient number of updates the persistent current will disappear at any temperature. One should note in this connection that while the "pseudodynamics" of the Monte Carlo method does not correspond to the real evolution of the system in time, it reflects the metastability of the persistent current that one should encounter in real systems.

IV. ANALYSIS

Here we estimate the energy barrier for the quantum phase slip associated with the unbinding of vortex-antivortex pairs in a system of finite size. The energy of a vortex pair has the form

$$E(r) = 2E_c + 2\pi\rho(T)J \ \ln(r/a), \tag{21}$$

where $E_c \sim J$ is the vortex core energy, a is the lattice spacing, r is the distance between the singularities in the pair, and $\rho(T)$ is helicity that describes the softening of the system with increasing temperature, $\rho(0) = 1$. Since the energy of the

pair increases with the distance, the unbinding takes place in one of two cases: (1) r reaches the linear size of the system $L = a\sqrt{N}$; (2) r reaches $r^* = a/\sqrt{f_V}$, the average distance between singularities. In the latter case realized for $r^* \lesssim L$, vortices and antivortices, after reaching this distance, recombine with the members of other pairs, which facilitates the phase slips. The vorticity and r^* can be estimated as

$$f_V = e^{-2E_c/T}, \quad r^* = ae^{E_c/T}. \tag{22}$$

For $r^* \lesssim L$ the barrier ΔE for the unbinding is given by $E(r^*)$,

$$\Delta E = E(r^*) = 2E_c + \frac{2\pi\rho(T)JE_c}{T}, \tag{23}$$

where the second term is dominant at lower temperatures. One can see that ΔE is independent of the system size. In this case the rate of the vortex-pair unbinding and, thus, the probability of the phase slip, are proportional to

$$\exp\left(-\frac{\Delta E}{T}\right) \cong \exp\left(-\frac{2\pi\rho(T)JE_c}{T^2}\right). \tag{24}$$

This result is independent of the system size. Thus one has to conclude that there is no spontaneous ordering and the supercurrent is zero in the half-fluxon case. However, because of the extremely low probability of current switching at low temperatures, a prepared state with supercurrent is a long-lived metastable state and it is practically impossible to obtain numerically the equilibrium result $I = 0$.

For systems of smaller size at low temperatures there are too few vortices, so that $r^* > L$ and the barrier is given by

$$\Delta E = 2E_c + 2\pi\rho(T)J\ \ln(L/a). \tag{25}$$

With the second term dominant, this leads to the phase slip (unbinding) rate proportional to

$$\exp\left(-\frac{\Delta E}{T}\right) \cong \left(\frac{a}{L}\right)^{2\pi\rho(T)J/T} = \frac{1}{N^{\pi\rho(T)J/T}}, \tag{26}$$

which decreases with the system size. One can see in Fig. 9(a) that for small sizes $I(T^*)$ is shifting to the right in accordance with Eq. (26) and then saturates in accordance with Eq. (24).

V. DISCUSSION

We have studied the dependence of the persistent current in a Josephson junction ring on the strength of quantum fluctuations, U/J, the number of superconducting islands, N, and the flux threading the ring, $\phi = \Phi/\Phi_0$. All three parameters can be controlled in experiment. The strength of quantum fluctuations is determined by the Josephson coupling of the islands and their capacitances. At some critical U/J the system undergoes a quantum phase transition into the superinsulator state characterized by zero conductivity of the ring in the presence of the superconductivity of the islands. Persistent current presents a good experimental tool for the investigation of this transition.

From a theoretical perspective the problem allows accurate numerical studies by Monte Carlo techniques developed for spin systems because it maps onto a classical 2D xy model at finite temperature. In this approach the critical strength of quantum fluctuations projects onto the temperature of the Kosterlitz-Thouless phase transition. The numerical solution of the problem is, however, significantly more challenging than equilibrium problems of spin physics because the persistent current disappears in the thermodynamic limit $N \to \infty$.

In accordance with the expectation we find that in all cases the persistent current is destroyed by sufficiently strong quantum fluctuations. The manner in which it is destroyed depends strongly on the number of superconducting islands in the Josephson junction ring and on the magnetic flux threading the ring. In cases of a half-integer flux, $\phi = n + 1/2$, when the classical ground state of the ring is degenerate, quantum fluctuations of any strength in theory destroy the persistent current. However, the phase slips required for that have a finite probability that is exponentially small at $U \ll J$. In that sense, the persistent current in the presence of weak quantum fluctuations is as stable as the magnetic moment of a superparamagnetic particle below the blocking temperature. Unlike the magnetization of a superparamagnetic particle (or of a finite-size Ising system) though, the persistent current cannot be made stable by increasing the system size. This is because the barrier for the switching of the current due to the quantum phase slip becomes size independent for large sizes. For small Josephson rings, we find that quantum fluctuations destroy the persistent current even faster. However, the dependence on the size is at best logarithmic. This finding can be of interest to the experimentalists.

When the classical ground state is not degenerate, the persistent current has a nonzero equilibrium value. At $U \ll J$ the spin-wave approximation provides excellent agreement with the numerical data on how the persistent current decreases when the strength of quantum fluctuations increases. The behavior is independent of the size of the ring. This prediction of the theory would be interesting to test in a real experiment. Another interesting prediction is that the departure from the universal behavior towards the behavior that depends on the size of the ring begins at the critical strength of quantum fluctuations determined by the bulk Kosterlitz-Thouless temperature. We present a numerical study of the phase slips due to the unbinding of vortex-antivortex pairs and analytical arguments that explain the size dependence of the persistent current. Our analysis supports conjecture of Ref. [8] that interaction between vortex-antivortex pairs on increasing U/J facilitates the phase slips.

ACKNOWLEDGMENTS

This work has been supported by Grant No. DE-FG02-93ER45487 funded by the US Department of Energy, Office of Science.

[1] See, e.g., S. L. Sondhi, S. M. Girvin, J. P. Carini, and D. Shahar, Continuous quantum phase transitions, Rev. Mod. Phys. **69**, 315 (1997).

[2] S. Sachdev, *Quantum Phase Transitions* (Cambridge University Press, Cambridge, UK, 2011).

[3] L. B. Ioffe, M. V. Feigel'man, A. Ioselevich, D. Ivanov, M. Troyer, and G. Blatter, Topologically protected quantum bits using Josephson junction arrays, Nature (London) **415**, 503 (2002).

[4] S. Gladchenko, D. Olaya, E. Dupont-Ferrier, B. Douçot, L. B. Ioffe, and M. E. Gershenson, Superconducting nanocircuits for topologically protected qubits, Nat. Phys. **5**, 48 (2009).

[5] V. E. Manucharyan, J. Koch, L. I. Glazman, and M. H. Devoret, Fluxonium: Single Cooper-pair circuit free of charge offsets, Science **326**, 113 (2009).

[6] A. D. Zaikin, D. S. Golubev, A. van Otterlo, and G. T. Zimanyi, Quantum Phase Slips and Transport in Ultrathin Superconducting Wires, Phys. Rev. Lett. **78**, 1552 (1997).

[7] D. S. Golubev and A. D. Zaikin, Quantum tunneling of the order parameter in superconducting nanowires, Phys. Rev. B **64**, 014504 (2001).

[8] G. Rastelli, I. M. Pop, and F. W. J. Hekking, Quantum phase-slips in Josephson junction rings, Phys. Rev. B **87**, 174513 (2013).

[9] R. M. Bradley and S. Doniach, Quantum fluctuations in chains of Josephson junctions, Phys. Rev. B **30**, 1138 (1984).

[10] S. E. Korshunov, Effect of dissipation on the low-temperature properties of a tunnel-junction chain, Zh. Eksp. Teor. Fiz. **95**, 1058 (1989) [Sov. Phys. JETP **68**, 609 (1989)].

[11] E. Chow, P. Delsing, and D. B. Haviland, Length-Scale Dependence of the Superconductor-to-Insulator Quantum Phase Transition in One Dimension, Phys. Rev. Lett. **81**, 204 (1998).

[12] See review and references therein: J. E. Mooij, G. Schön, A. Shnirman, T. Fuse, C. J. P. M. Harmans, H. Rotzinger, and A. H. Verbruggen, Superconductor-insulator transition in nanowires and nanowire arrays, New J. Phys. **17**, 033006 (2015).

[13] See, e.g., G. Schwiete and Y. Oreg, Persistent Current in Small Superconducting Rings, Phys. Rev. Lett. **103**, 037001 (2009), and references therein.

[14] K. A. Matveev, A. I. Larkin, and L. I. Glazman, Persistent Current in Superconducting Nanorings, Phys. Rev. Lett. **89**, 096802 (2002).

[15] M. Y. Choi, Persistent current and voltage in a ring of Josephson junctions, Phys. Rev. B **48**, 15920 (1993).

[16] M. Lee, M.-S. Choi, and M. Y. Choi, Quantum phase transitions and persistent currents in Josephson-junction ladders, Phys. Rev. B **68**, 144506 (2003).

[17] I. M. Pop, I. Protopopov, F. Lecocq, Z. Peng, B. Pannetier, O. Buisson, and W. Guichard, Measurement of the effect of quantum phase-slips in a Josephson junction chain, Nat. Phys. **6**, 589 (2010).

[18] M. Tinkham, *Introduction to Superconductivity* (Dover, New York, 2004).

[19] J. R. Friedman, V. Patel, W. Chen, S. K. Tolpygo, and J. E. Lukens, Quantum superposition of distinct macroscopic states, Nature (London) **406**, 43 (2000).

[20] C. H. van der Val, A. C. ter Haar,F. K. Wilhelm, R. N. Schouten, C. J. Harmans, T. P. Orlando, S. Lloyd, and J. E. Mooij, Quantum superposition of macroscopic persistent-current states, Science **290**, 773 (2000).

[21] S. Chakravarty, G.-L. Ingold, S. Kivelson, and A. Luther, Onset of Global Phase Coherence in Josephson-Junction Arrays: A Dissipative Phase Transition, Phys. Rev. Lett. **56**, 2303 (1986).

[22] M. Wallin, E. S. Sørensen, S. M. Girvin, and A. P. Young, Superconductor-insulator transition in two-dimensional dirty boson systems, Phys. Rev. B **49**, 12115 (1994).

[23] K. Kim and D. Stroud, Quantum Monte Carlo study of a magnetic-field-driven two-dimensional superconductor-insulator transition, Phys. Rev. B **78**, 174517 (2008).

[24] J. Tobochnik and G. V. Chester, Monte Carlo study of the planar spin model, Phys. Rev. B **20**, 3761 (1979).

[25] R. Gupta and C. F. Baillie, Critical behavior of the two-dimensional XY model, Phys. Rev. B **45**, 2883 (1992).